Materials Today Sustainability 34 (2026) 101376

Contents lists available at ScienceDirect

Materials Today Sustainability

journal homepage: www.journals.elsevier.com/materials-today-sustainability

Hemp fines as alternative lignocellulosic material for non-woven semi-rigid thermal insulation panels

Percy Alao [a,*], Maximilien Gibier [b], Silvia Bibbo [a], Laurent Bedel [b], Stergios Adamopoulos [a]

[a] Department of Forest Biomaterials and Technology, Swedish University of Agricultural Sciences, Uppsala, Sweden
[b] SOPREMA, 15 rue de Saint Nazaire, Strasbourg, 67100, France

ARTICLE INFO

Keywords:
Hemp fines
Sustainable materials
Insulation
Thermal conductivity
Particle size analysis
Chemical composition

ABSTRACT

The incorporation of sustainable materials such as hemp fines, approximately 6 wt% of the byproduct generated from hemp processing, into thermal insulation panels present a promising opportunity for enhancing energy efficiency in construction. These hemp fines were characterized and incorporated with wood fibres at substitution rates of 25%, 50%, and 100% by mass to develop semi-rigid thermal insulation panels. The thermal and functional properties of the panels were evaluated to determine the optimal substitution rate. The findings revealed that shorter hemp fines have a high soluble content (23%), low thermal stability, and increased moisture sorption. A 25% substitution with short hemp fines (90th percentile length of 5.8 mm) resulted in panels that perform comparably to those made from wood fibres (90th percentile length of 6.2 mm). For applications that prioritize low thermal conductivity, a 50% substitution with either type of hemp fine (short, super-short) proved effective. Notably, panels with super-short fines (90th percentile length of 3.3 mm) exhibited the best homogeneity and internal bond strength (2.5 kPa), although the high moisture sorption, highlighted for the fines, raises concerns about panel durability. In conclusion, this study demonstrates the viability of using hemp fines in the production of sustainable insulation and recommends a 25% substitution rate for a balanced set of properties.

1. Introduction

The increasing variety of environmental restrictions and requirements from policymakers is driving a surge in demand for renewable and biodegradable materials [1]. Since 1970, economic activities have tripled the extraction and processing of natural resources, contributing to approximately 50% of greenhouse gas (GHG) emissions [2]. This has led to environmental concerns, particularly regarding climate change and resource depletion [3]. The building sector is a major contributor to this problem, accounting for 20–40% of the total energy consumption and nearly 33% GHG emissions in the EU [4,5]. Buildings also account for approximately 25% of global water consumption [5]. Consequently, prioritising the building sector is crucial for reducing resource consumption and associated CO_2 emissions [6].

Building materials, particularly insulation, are indispensable for achieving energy savings [7]. While conventional materials like polystyrene, polyurethane, glass, and rock wool are widely used, their production is often energy intensive [7]. Besides, a recent study [8] noted that conventional insulation materials, such as polyurethane, have a significant disadvantage due to their high flammability and the release of toxic gases (highly poisonous hydrogen cyanide and isocyanates [9]) during combustion. These shortcomings have led to a growing interest in natural materials. Studies have examined plant-based materials like hemp, wood fibres, and flax as alternative materials for conventional materials in terms of thermal insulators [10–12]. These biomass-derived materials are a more environmentally acceptable alternative, as they can mitigate GHG emissions, require less energy to produce, and improve indoor air quality [13]. In addition to biomass fibres, several studies [14,15] have highlighted advancements in thermal insulation using novel materials such as aerogels. These materials have demonstrated a thermal conductivity range of 0.009 to 0.040 W/(m.K), which is better than or comparable to that of conventional insulation materials. Other research have focused on nanosized fibrous materials developed through nanotechnology engineering, which can achieve thermal insulation potential as low as 0.015 W/(m·K) [16]. Despite their impressive performance, these advanced materials are not yet widely adopted for mainstream

* Corresponding author.
E-mail addresses: percy.alao@slu.se (P. Alao), mgibier@soprema.fr (M. Gibier), silvia.bibbo@slu.se (S. Bibbo), lbedel@soprema.fr (L. Bedel), stergios.adamopoulos@slu.se (S. Adamopoulos).

https://doi.org/10.1016/j.mtsust.2026.101376
Received 8 October 2025; Received in revised form 22 December 2025; Accepted 24 April 2026
Available online 27 April 2026

building insulation. This is mainly due to challenges such as high costs and logistical difficulties. However, they are becoming more viable for specialised and high-performance applications in industrial settings.

Although natural materials offer numerous benefits as thermal insulation materials, achieving greater circularity in construction is crucial. Reusing and recycling materials helps reduce the consumption of non-renewable resources, minimises landfill waste, and reduces embodied carbon emissions [17], but also improve natural resource efficiency. As an important segment of the construction sector, the construction insulation market is estimated to increase at a compound annual growth rate of 4.5% up to 2027 [18]. This trend highlights the significant potential for innovative materials. To break the link between economic activities and resource depletion, adopting a circular economy approach is essential [19]. This approach involves repurposing waste generated from natural material processes to create closed resource loops.

Hemp is identified as a key resource for a circular economy due to its potential as a sustainable crop for various materials [20], including thermal insulation [21–24]. According to Agrawal, and [25], hemp is a natural biomass with considerable prospect as a sustainable crop for developing various materials to substitute existing industrial and consumer products. However, aside from the fibres generated from the hemp stalk, most research, including studies by Latif, Tucker [26] and Kolak and Oltulu [27], focuses on the use of whole biomass stalks or shives. To fully align with circular economy principles, there is a pressing need to repurpose hemp fines, a major waste fraction from the processing of hemp stalks, particularly since hemp fibres have become prominent for composites development in automotive applications.

This study aims to address this research gap by exploring the potential of hemp fines as a valuable resource for novel insulation materials. Insulation applications for the hemp fines are particularly seen as a feasible means to effectively repurpose these wastes, considering that hemp-based insulation has been reported with strong performance across environmental and economic indicators like global warming, carbon offset, and soil organic carbon compared to extruded polystyrene foam (XPS), and outperforms gypsum and plywood in terms of energy and land use [28]. During the processing of hemp stalks to obtain technical fibres (such as automotive fibres) in industries like BAFA Neu GmbH, fractions like shives, hemp fines (super-short and short fibres), and dust constitute a notable portion of the material produced. While hemp shives have already garnered significant research interest and applications, much less attention has been placed on the fines.

The novelty of this research lies in its focus on the valorisation of hemp fines, an underutilised by-product of the hemp industry, to address a growing market need. While hemp insulation materials are not new, the successful conversion of this low-value waste material into a high-value thermal insulation product provides a compelling example of a circular bio-based economy in action. Hemp fines possess several beneficial physical properties essential for insulation. They have a low bulk density, which increases air entrapment and is crucial for achieving low thermal conductivity [29]. Additionally, they have a porous cellular structure that minimises heat conduction. Chemically, hemp fines may have a high lignin content due to the lignin-rich core layer [30]. This high lignin content increases the potential for charring [31–33], thus providing a degree of fire resistance. Additionally, this suggests increased hydrophobicity and, consequently, reduced water affinity. Nevertheless, the material's hygroscopic nature is also essential. Its capacity to absorb and release moisture is critical for sustained sorption performance and plays a significant role in enhancing indoor air quality [16,34,35].

Most notably, this study specifically investigates a newly developed thermal insulation panel made from a combination of hemp fines and softwood fibres. The research focuses on synergistically combining the biomass to address the unique challenges and opportunities presented by the small particle size of the fines and to achieve an optimal blend. This approach provides a sustainable alternative to synthetic insulation materials, helping to establish a new value chain for thermal insulation products and promoting the use of renewable, biodegradable materials.

2. Materials and methods

2.1. Materials

2.1.1. Hemp fines

Hemp fines, including short fibres (KF) and super-short fibres (SKF), are generated (Fig. 1(a)) as by-products during the production of technical hemp fibres (*Cannabis sativa* L. cv. Finola2) by BAFA Neu GmbH (Malsch, Germany). The feedstock consisted of various degrees of retted (slightly retted and well retted) hemp stems. The hemp straws were obtained from seeds sowed in May 2024. The hemp stems were approx. 450–600 mm long after chopping. The dried stocks were passed through a machine in a process known as mechanical scutching that removes the outer bark and woody core, leaving the long bast fibres (shives). No specific regards are paid to the ratio of retting in the feedstock. Fig. 1(b) shows the fractions of materials generated following the processing of the hemp stems into technical fibres. For every 1000 kg of hemp stems processed into technical fibres, approximately 20 kg and 40 kg of SKF and KF are produced. The current pilot site (Waldhegenich, Bühl, Germany) for the hemp biomass cultivation generates about 8000 kg of hemp straw from 1000 kg of hemp seeds planted per hectare. This implies that the yield of KF and SKF is notable, with approximately 320 kg and 160 kg, respectively.

2.1.2. Wood fibres

The base material for thermal insulation panels is refined softwood fibres from SOPREMA (Golbey, France) to which hemp fractions are added. The fibres were obtained using Thermo-Mechanical Pulping (TMP) defibration of industrial softwood chips (mainly spruce, fir, and other softwoods available around the industrial plant). The softwood chips are supplied within a maximum 200 km radius of the industrial plant and are made from thinning logs and sawmill by-products. The detailed process parameters are confidential.

2.1.3. Bicomponent binder

The binder is bicomponent fusible fibres, made of a core material and a shell that exhibits a melting temperature lower than the core one. The bicomponent fibres chosen for the study are the same as the industrially used fibres for SOPREMA's regular semi-rigid insulation batts, enabling a direct comparison with conventional industrial batts.

2.2. Methods

2.2.1. Analysis of biochemical components

The biochemical composition of the biomass was assessed by measuring the content of cellulose, hemicelluloses, and lignin, along with thermal properties and crystallinity.

2.2.1.1. Chemical composition. Chemical composition of the biomass was determined by the Van Soest method, as previously applied in other studies Marrot et al. (2021). The biomass (1 g of grinded oven-dried samples) was treated with three detergent solutions followed by calcination. The first treatment involved Neutral Detergent Fibre (NDF) extraction, which partially removed pectins. The NDF solution consisted of 30 g/L sodium dodecyl sulfate, 18.61 g/L ethylenediaminetetraacetic acid (EDTA), 6.81 g/L sodium borate, and 4.56 g/L disodium hydrogenphosphate dihydrate. The second stage, Acid Detergent Fibre (ADF) extraction, removes pectins and hemicelluloses. The ADF solution contained 20 g/L cetyl trimethylammonium bromide in 0.5 M H_2SO_4. Each extraction was conducted for 1 h at 100 °C. The fines were thoroughly rinsed three times with boiling water and then with acetone. The Acid Detergent Lignin (ADL) extraction of ADF residues involved an acidic

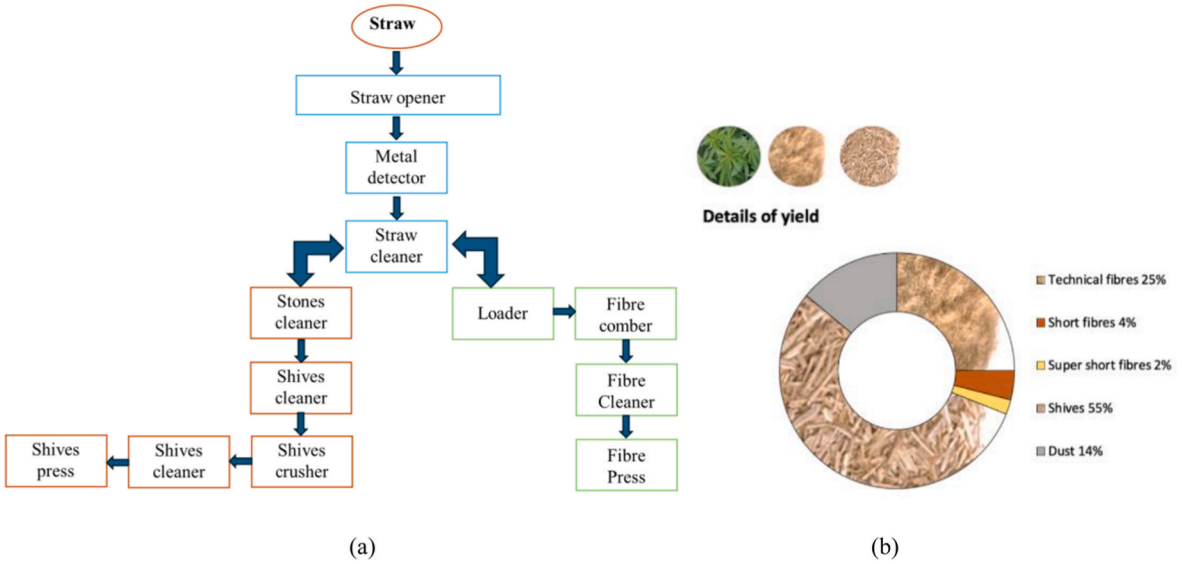

Fig. 1. (a) The schematic of fibres and fines generation; **(b)** details of fines (short fibres (KF) & super-short fibres (SKF)) yield compared to technical fibres following mechanical decortication of hemp stems (BAFA Neu GmbH).

solution of 72% H_2SO_4 (12 M) to remove cellulose. The final calcination step was done by incinerating the ADL residues in a furnace for 2 h at 550 °C. By monitoring the mass loss during these successive specific attacks, it was possible to estimate the cellulose, hemicelluloses, soluble content (primarily pectins), lignin, and ash (inorganic matter) contents.

2.2.1.2. Crystallinity (X-ray diffraction). X-ray diffraction (XRD) was performed with a Malvern PANalytical Empyrean diffractometer equipped with a Cu LFF HR X-ray tube and a PIXcel3D detector. The diffraction pattern was obtained between 10° and 35° (2θ angle range) using diffracted intensity of Cu (1.5405 Å) to obtain maximum intensity of diffraction of the (002), i.e., $I_{002,}$ the intensity of the lattice at 2θ angle, between 22° and 23° and I_{am} for the amorphous contents at 2θ angle, between 18° and 19°. Crystallinity index (I_c, %) was then estimated based on the Segal method, see equation below:

$$I_C = 100 \times \frac{I_{002} - I_{am}}{I_{002}}$$

Furthermore, the crystallite size (D) was calculated using the Scherrer formula, as shown in the equation below. This method for estimating crystallite size has been used and discussed in numerous studies, including those by Hassanzadeh-Tabrizi [36], Salem, Kasera [37], Wang, Chang [38], French and Santiago Cintrón [39], Qinglin, Jinquan [40], Newman [41].

$$D = \frac{K\lambda}{\beta \cos \theta}$$

where K is Scherrer's constant (0.9), λ (0.15406 nm) is wavelength of radiation for Cu, β is the full width at the half maximum of diffraction peak in radians, and θ is Bragg's angle (2θ/2) in radians.

Thermogravimetric analysis (TGA). The analysis was done using a Mettler Toledo analyser TGA2 (Mettler Toledo, Greifensee, Switzerland), under a nitrogen atmosphere with a flow rate of 20 mL/min. Samples were milled using a Retsch SM100 mill to pass a 40-mesh screen. Roughly 6 mg of oven-dried granules were put in a standard TGA alumina crucible pan. The analysis started with a 5-min isothermal segment at 27 °C, followed by a dynamic heating stage to 600 °C at a rate of 5 °C/min, and concluded with a final 5-min isothermal stage at 600 °C.

2.2.2. Analysis of the biomass physical properties

Particle size and moisture behaviour of the biomass were assessed to understand their critical impact on insulation panel performance. An unsuitable particle size affects processability, density, and thermal conductivity, while moisture behaviour is key to a panel's thermal performance, durability, and stability.

2.2.2.1. Size analysis. The size analysis was achieved using a dynamic image analysis system QICPIC (Sympatec, GmbH, Clausthal-Zellerfeld, Germany) equipped with a FIBROS feeder for dry dispersion. The system provided various size and shape parameters, including GRADIS (Gradient Intensity Size). The fibre counts per sample was about 63430. The analysis was done based on volume and performed with a measuring range of 17 μm to 33792 μm. The volumetric approach for the fibre size distribution was applied due to the bulk nature of the materials.

2.2.2.2. Dynamic vapour sorption (DVS). The analysis was performed on granulates (20 ± 2 mg) using a DVS-ET-VID by SMS (Surface measurement systems, London, UK). The samples were oven dried before the analysis. Both adsorption and desorption were examined with relative humidity (RH) from 10% to 95% (at intervals of 10%, but 5% in the steps 90–95% RH) and temperature of 25 °C.

2.2.3. Fabrication of semi-rigid insulation panels

The KF and SKF were prototyped on SOPREMA pilot line with representative performances of the industrial line panels to produce semi-rigid insulation panels of 55 kg/m^3 density and a dimension of 250 × 250 mm^2. The base material of the panels is wood fibre from SOPREMA to which hemp fine fractions were added based on the incorporation rate shown in Table 1.

The fabrication process is illustrated in Fig. 2. It describes the transition of material to product through four main components.

Table 1
Description of fabricated samples.

Type of material	Incorporation rate		
	25%	50%	100%
Softwood fibres (wood_ref)	-	-	✓
Hemp short fibres (KF)	✓	✓	✓
Hemp super-short fibres (SKF)	✓	✓	-

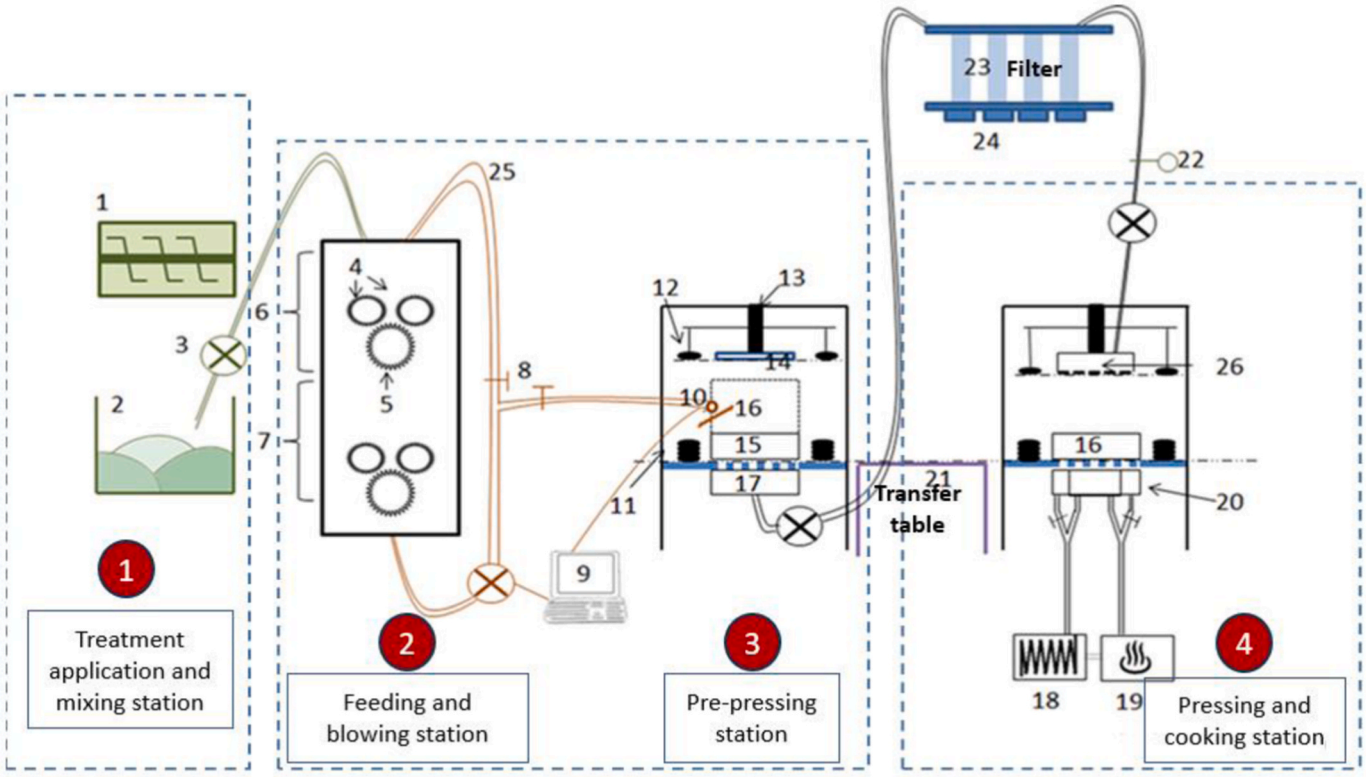

Fig. 2. Production stages of semi-rigid prototype panels.

1. A feeding tower prepares the fibres, including bicomponent polymer fibres, by blowing a homogeneous mixture into the mould. The feeding tower utilises several fans and spiked rolls that open and homogenise the fibre mix through appropriate operational settings. The quantity of bicomponent fibres remained the same as in the reference regular 100% wood panels. To achieve the desired fire performance, a fire retardant based on an ammonium salt was added. The specific rate and formula are confidential.
2. A pre-pressing station to reduce the thickness of the blend, as on an industrial line. The pre-pressing station also includes a fan that cools the panels at the end of cooking. The blend is mechanically pre-pressed before being transferred to the cooking station.
3. A press that allows for blowing a stream of hot air for semi-rigid panels. Cooking was done at atmospheric pressure. Hot air, produced by a hot air generator, flows through the panel through openings in the press plate. The direction of air flow can be changed—either from bottom to top or from top to bottom—during baking to ensure even baking of the panel.
4. The press has internal dimensions of approximately 600 mm × 600 mm. The mould used has dimensions of 270 mm × 270 mm. A panel height of 100 mm can be reached only for low density panels, because of the fluffiness of fibres. The press has a heating chamber blowing hot air at roughly 140 °C to the mix for approximately 8 min to enable sufficient wetting by the

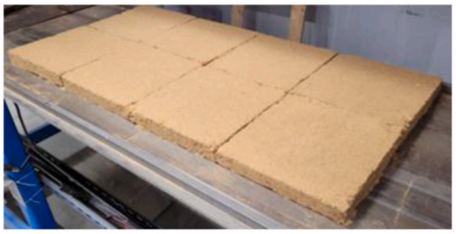

(a)

(b) (c)

Fig. 3. Rigid insulation board prototypes with 100% incorporation of **(a)** wood fibres; **(b)** short hemp fibres; and **(c)** super-short hemp fibres.

bicomponent fibre. The non-woven panels are pressed to a targeted thickness of 40 mm. The panel is then cooled in the pre-pressing station, which incorporates a fan to extract heat from the panel.

The recipe developed by SOPEREMA is specific to the machine (valve opening rate, air flow direction, air flow temperature) to obtain representative performances of the semi-rigid industrial line panels.

Fig. 3 presents the 100% batch of the panels. The 100% semi-rigid panels from SKF fibres (Fig. 3(c)) did not produce acceptable results due to easy deformation, and lower thickness (29 mm).

2.2.4. Characterization of the insulation panels

A comprehensive analysis of the thermal insulation panels was performed to assess different critical aspects of the panels' function and reliability, such as tensile resistance (internal bond strength), dust content, reaction to fire properties, and thermal insulation performance. These analyses are essential for a thermal insulation panel moving from raw material conceptualization to a verified, safe, and effective product that fulfils industrial-relevant requirements.

2.2.4.1. Tensile resistance. The tensile resistance to surface test (internal bonding) was performed in accordance with EN 1607. Three (3) samples with sample size: 200 × 200 mm^2 were examined per batch. Conditioning of the panels was done prior to testing at 23 °C/50% RH. The tensile test was done with GALDABINI Quasar (Varese, Italy) equipped with a 25 kN load cell. The test was done at a rate of 10 mm/min.

2.2.4.2. Dust content. The test consists of aggravating/shaking the samples to extract dust or unbound particles. A sample with size: 200 × 200 mm^2, conditioned at 23 °C and 50% RH, was examined.

2.2.4.3. Reaction to fire properties. A flame test was performed according to EN ISO 11925-2 (Fire reaction test. Flammability test of building products under direct flame exposure. Part 2. Test with a single flame source). The test examines whether the flame tip reaches 150 mm above the flame application point (flame height (Fs)). This test is a mandatory step in classifying construction products based on European EN 13501-1 classes E (Fs ≤ 150 mm with 20 s exposure) and F (no performance determined). Four (4) replicates and 8 faces were tested using samples of 250 × 90 mm^2, following conditioning at 23 °C and 50% RH.

2.2.4.4. Thermal insulation performance. The test was done on dried samples, using a HESTO HLC T520 (HESTO Elektronik GmbH, Germany), based on EN 12667. Two (2) samples (250 × 250 mm^2) were examined per batch.

3. Results and discussion

3.1. Composition and structure of the biomass (wood fibre and hemp fines)

3.1.1. Biochemical composition

Table 2 presents the chemical composition of the fibres from softwood (wood_ref) and hemp fines (short hemp (KF) and super-short hemp (SKF)). The result indicates a notable variation between the hemp and wood biomass. SKF shows greater overall soluble content and the high variation in cellulose and lignin. The notable difference between the lignin content of KF and SKF is because SKF comprises a high amount of the core layer of the stem (xylem), which is reported in literature [42] to contain a high concentration of lignin. In contrast, KF is mainly comprised of outer fibres of the stalk that are mainly reach in cellulose. To our knowledge, studies have not exclusively examined the biochemical composition of such hemp fines. However, the composition of SKF, closely aligns with that of hemp woody core reported by Bokhari, Chi [43]. The study noted that cellulose, hemicellulose, and lignin levels varied from 40% to 48%, 18% to 24%, and 21% to 24%, respectively, when compared with bast fibre. The high variation in lignin content measured for SKF indicates a heterogeneous by-product since it is a mixture of fragmented components from two main parts of the hemp stalk, each with a very different lignin content. Following the mechanical process to remove the long fibres, primarily from the fibrous outer layer (phloem), which is cellulose rich, the residue is characterised by inner woody core (xylem) that is notably rich in lignin. The hemp stems go through a breaking process that generates the fines and shorter fibres, which are largely in the core layers of the plant. Mechanical scutching further separates the fibres from the hurds, producing more fines in the process. This outcome has been previously highlighted in past research [30]. The chemical composition of the technical hemp fibres (longer fibres) from the same hemp stalk showed a cellulose and hemicelluloses content similar to KF (approximately 71% and 7%, respectively). Furthermore, the composition of these components in KF closely correlates with values reported for long fibres in the literature [44], particularly for hemicelluloses [45]. This suggests that KF fines differ from technical fibres mainly in their length and contain less woody core than SKF.

3.1.2. XRD

In Fig. 4, the prominent peak observed at 2θ = 22.6° (SKF), 22.7° (wood_ref), and 22.8° (KF) corresponds to the (002) crystallographic plane, a characteristic reflection of cellulose Iβ. The subtle shifts in the (002) peak position reflect minor variations in the cellulose crystal lattice among the samples, potentially arising from compositional differences, crystallite size variations, or lattice strains. Therefore, the 2θ value for KF indicates a decrease in the distance between atomic planes, signifying a more packed crystalline structure. This tighter packing in KF is consistent with its high crystallinity index (Table 3) and highlights the distinction in amorphous content compared to other materials, as non-cellulosic components like soluble content, hemicelluloses, and lignin are known to reduce crystallinity [46,47]. The intensity of I_{am} is lowest in KF and highest in the wood reference, suggesting a higher overall amorphous fraction in the wood reference material than SKF. This

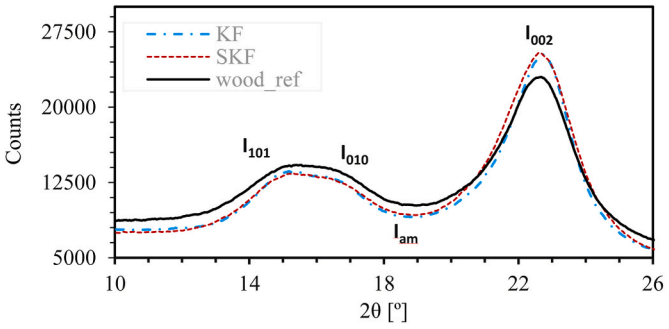

Fig. 4. X-ray diffraction patterns.

Table 2
Chemical composition comparison between hemp fines and SOPREMA reference wood.

Biomass	Pectin and soluble content, wt.%	Hemicelluloses, wt.%	Cellulose, wt.%	Lignin (acid insoluble), wt.%	Residual ash, wt.%
SKF	22.5 ± 3.0	10.9 ± 3.9	51.6 ± 9.1	21.6 ± 18.9	1.9 ± 1.2
KF	8.8 ± 1.8	9.7 ± 4.2	69.3 ± 3.4	6 ± 2.8	3.9 ± 1.5
wood_ref	7.6 ± 1.8	14.7 ± 0.9	48.3 ± 3.1	25.8 ± 1.6	6.1 ± 1.6

Table 3
Crystallinity index and crystallite size of the biomass.

Biomass	2θ (am), °	2θ (002), °	I_{am}, intensity	I_{002}, intensity	I_c, %	D, nm
SKF	19	22.6	9242	25399	63.6	3.85
KF	19	22.8	9040	25239	64.2	4.14
wood_ref	19	22.7	10204	22991	55.6	4.04

outcome may be due to the high variability in the lignin content measured for SKF. The crystallinity index measured for the hemp biomass aligns with some past studies though results vary. For instance, values of 62.5% were reported by Lawan, Argunam [48] and 69.7% for the Fedora variety was found by Marrot, Lefeuvre [49]. Müssig, Amaducci [44] highlighted the limitations of comparing XRD data from various studies due to variation in techniques but noted that the crystallinity index of hemp fibre bundles can range from 53 to 73%.

Regarding crystallite size (Table 3), a general positive correlation exists between cellulose Iβ crystallite size and crystallinity index [37]. The short hemp fines (KF) show a slightly larger estimate of crystallite size, which is consistent with their I_c. However, the roughly 0.3 nm difference between all the samples is within the typical range of variability for this type of estimation and is not considered substantial. Similar method of estimation of crystallite size in a study by Newman [41] has shown that the crystallite sizes of lignocellulosic materials can vary from 2.6 to 5.6 nm. The small crystallite size estimated in this study aligns with the broad peak observed in the X-ray diffraction pattern. A limitation of this estimation method, however, is that a high amorphous content influences the accuracy of pinpointing the correct baseline. This, in turn, affects the precision of the FWHM determination. The estimated crystallite size therefore only provides a basis for the comparative analysis of the biomass in the current study.

In terms of thermal insulation applications, a lower I_c can be beneficial due to the potential for lower thermal conductivity and higher porosity. However, lower I_c tends to indicate higher moisture affinity.

3.1.3. TGA

The thermal decomposition curves are presented in Fig. 5. All samples exhibited an initial mass loss (ML) below 100 °C, primarily attributed to the desorption of residual bound water and/or highly volatile extractives, despite prior oven-drying. Peak mass loss temperatures for this initial stage were approximately 62.6 °C for the wood reference, 83.2 °C for SKF, and 75 °C for KF. Corresponding average mass losses at these peaks were 0.7% for wood reference, 4% for SKF, and 3.2% for KF. The higher initial mass loss (4%) and raised peak temperature (83.2 °C) for SKF than KF and the wood_ref suggest a greater quantity of more tightly bound water and/or a higher content of volatile extractives (also observed in the sorption for desorption at 0% RH). As confirmed by chemical composition analysis, SKF contains a notable amount of these components, which would require specific thermal profiles for complete removal. To better understand the thermal decomposition profile from Fig. 5, we summarise and discuss the main decomposition temperature in Table 4.

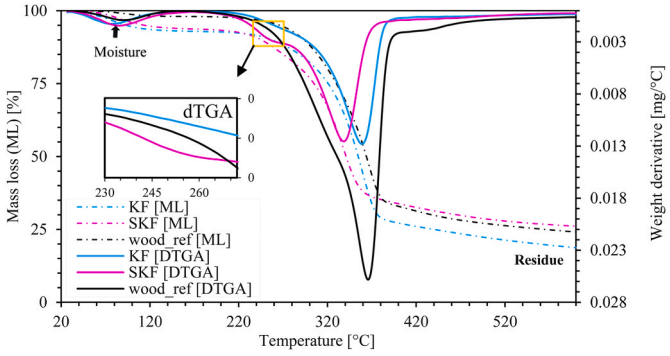

Fig. 5. TGA and dTGA curves of the wood reference and hemp fines.

Quantitatively, Table 4 shows that most components in SKF were lost below 100 °C, unlike KF and the wood reference, which demonstrated further cumulative mass losses of 1.1% and 2.3%, respectively, beyond their initial peak. This highlights a variation in components that require desorption at a wider temperature span up to 100 °C. The lower initial mass loss percentages observed at the respective peaks for KF and wood correlate with their reduced soluble content compared to SKF. However, their subsequent cumulative mass losses up to 100 °C (1.1% for KF and 2.3% for wood reference) indicate a more gradual or extended desorption of remaining low-temperature volatiles and/or bound water, even after their primary mass loss peaks. This implies that while their overall soluble/volatile content is lower than SKF's, the specific nature of their extractives, water binding affinities, or morphological structures influences their distinct desorption kinetics. Fig. 5 also shows notable differences in thermal degradation profiles for hemicelluloses decomposition region (200–350 °C) in the dTGA curve. SKF displayed a distinct hemicelluloses degradation peak from about 230 °C to 268 °C (highlighted in Fig. 5). In contrast, the wood reference showed a broader peak (250–320 °C), and KF exhibited a more smeared decomposition profile starting at a slightly higher temperature (~245 °C) than SKF. The differences in how biomass samples break down at this temperature range indicate the types of hemicelluloses they contain. For example, a study by Werner, Pommer [50] showed that different hemicellulose polysaccharides have varying thermal decomposition profiles. It reported that arabinoxylan has lower thermal stability. This suggests that SKF may contain more arabinoxylan than KF. There are also well-reported differences in the hemicelluloses of softwood and hemp, most critically in the xylan polysaccharide. Hemp xylans primarily comprise arabinoxylans and glucuronoxylans [51], which are more like hardwood xylan. Hardwood xylan is characterised by its overall composition, with a high proportion of O-acetyl-4-O-methylglucuronoxylans as the dominant hemicellulose. Softwood, such as the wood reference in this case, is composed predominantly of glucomannans, particularly arabinoglucuronoxylan, which is a type of arabino-4-O-methylglucuronoxylan [52]. According to Abik, Palasingh [53] the composition of this galactoglucomannan can vary from 16 to 17% in softwoods like spruce ((*Picea abies*) and (*Picea glauca*)).

The $T_{50\%}$ ML in Table 4 indicates that SKF exhibits lower overall thermal stability compared to KF and the softwood fibre. This trend is consistent with the measured cellulose contents in the SKF. However, despite having a lower cellulose content than the hemp fines, the reference wood demonstrates better overall thermal stability. As previously mentioned, the synergistic interactions between the biomass components are a key factor influencing several behaviours, including thermal properties. According to Apaydın Varol and Mutlu [54], the process of pyrolysis is still complex, and the explanations of each individual reaction or the synergetic effects of the components are not yet clear. While higher cellulose crystallinity and better organization are typically expected to enhance thermal stability, this was not the primary driver in this case. The results therefore suggest that despite the hemp fines' high cellulose content relative to the wood reference, the interplay among their components, notably SKF's high soluble content and KF's low lignin content, along with the specific types of hemicelluloses, likely creates a less thermally robust overall structure, leading to earlier

Table 4
The mass loss at 100 °C and the temperatures corresponding to 5% and 10% mass loss (ML) for untreated and treated hemp fibres.

Biomass	Mass loss up to 100 °C	$T_{5\%}$ ML, °C	$T_{10\%}$ ML, °C	$T_{50\%}$ ML, °C	Residue, %
wood_ref	1.8 ± 0.9	266 ± 6	291 ± 5	360 ± 7	22 ± 3.8
SKF	4.1 ± 2.5	145 ± 67	234 ± 24	341 ± 3	26 ± 2.8
KF	5.5 ± 2.0	116 ± 51	249 ± 36	355 ± 2	19 ± 1.8

component decomposition. This outcome aligns well with previous study by Long, Zhou [55], where an increase in cellulose decomposition temperature (342 to 362 °C) occurred, due to interactions between cellulose and xylan components. As previously noted, compositional variations in xylans between hemp fines and wood reference likely lead to differences in their linkages with cellulose and lignin within the cell wall. According to Berglund, Mikkelsen [56], unlike the network in hemp, xylans commonly form covalent bonds with lignin in wood, which provides a stronger protective effect around cellulose microfibrils. This linkage can indirectly enhance the thermal stability of associated cellulose, shifting its main degradation peak to higher temperatures. This is consistent with the observed degradation profile (Fig. 5) where the sharper, more distinct hemicelluloses peak, particularly for SKF, suggests a less robust link between hemicelluloses and lignin, indicating minimal interference from broader lignin degradation in that range. Besides, the compositional analysis already detailed a higher overall proportion of hemicelluloses in the wood reference compared to the hemp fines. Therefore, the optimal thermal stability of a lignocellulosic material depends not only on the quantity or intrinsic quality of its cellulose (or crystallinity), but also on cellulose's protective environment and the overall matrix structure.

Inorganic residue from TGA analysis provides information on the potential inherent fire resistance of a biomass. Even though SKF showed higher inorganic residues than KF and wood reference, this was found to be statistically non-significant (P-value = 0.076). Therefore, this particular outcome likely suggests that any variation in the reaction to fire behaviour of the biomass is less likely due to the inorganic composition.

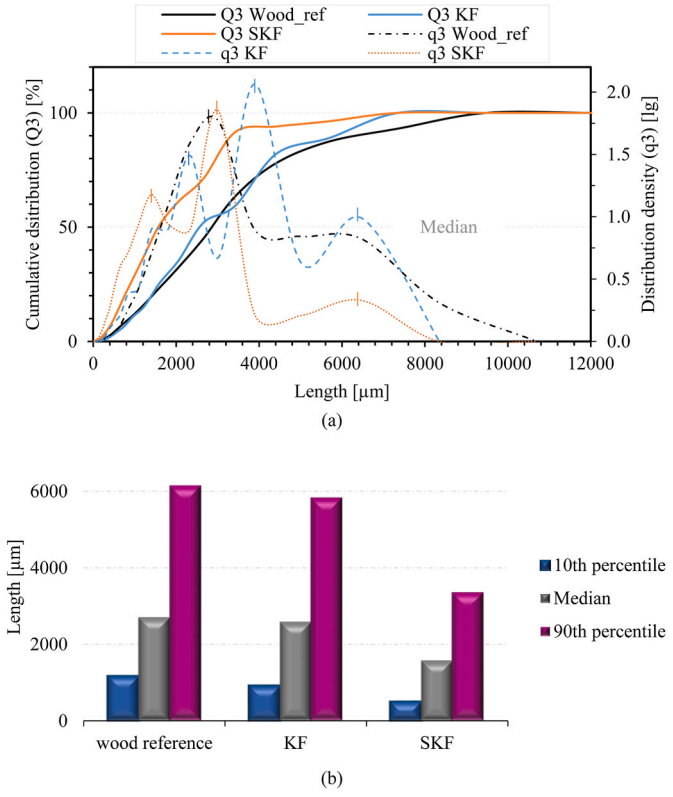

Fig. 6. (a) The length cumulative distribution (Q) and density distribution (q); **(b)** 10th percentile, median and 90th percentile fibre length of softwood reference fibres and hemp fines (short hemp (KF), super-short hemp (SKF)).

3.2. Physical properties

3.2.1. Particle size analysis

Fig. 6(a) presents the particle size distribution of the three investigated materials: wood_ref, KF, and SKF. Both the cumulative distribution (solid lines) and the distribution density (dashed lines) are reported to provide a comprehensive description of particle size characteristics. The cumulative distributions show distinct differences among the samples. SKF exhibits a swift initial increase at shorter fibre lengths (<1000 µm) compared to KF and the wood_ref. This suggests that SKF contains a markedly higher percentage of fibres shorter than 1 mm, as evidenced by the 10th percentile of volume size being below 0.5 mm and a median volume length of 1.57 mm (Fig. 6(b)). In contrast, the median volume length for KF and the wood_ref are 2.59 mm and 2.71 mm, respectively. Furthermore, 40% of the fibres in SKF (those between the median and the 90th percentile) fall within the length range of 1.57 mm to 3.36 mm. This contrasts with the corresponding 40% ranges of 2.59 mm–5.84 mm for KF and 2.71 mm–6.15 mm for wood_ref. Consequently, only 10% of the total volume of SKF exceed the length of 3.4 mm (the 90th percentile), while the maximum corresponding lengths for KF and wood_ref are 5.8 mm and 6.2 mm, respectively. Notably, the maximum particle length for the wood_ref is roughly 9 mm, while KF and SKF have maximum lengths of 7.2 mm and 7 mm, respectively.

The distribution density curves highlight additional size differences. The wood_Ref displays a bimodal distribution, with a dominant peak around 3.0 mm and a secondary, much smaller broad peak between 5 and 8.3 mm. KF and SKF exhibit multimodal distributions, reflecting multiple particle subpopulations. SKF shows distinct peaks around 1.4 mm, 3.0 mm, and a small peak at about 6.5 mm. In contrast, KF has peaks near 2.3 mm and 4.0 mm, with a much larger proportion of particles at 6.5 mm. KF presents slightly higher relative proportions of both fines and longer particles compared to wood_ref, making it a more variable material, although still within a similar size range. SKF, in contrast, has a dominant peak slightly above 2.0 mm and a sharp decline above 3 mm, confirming its overall finer and narrower fibre size.

From a processing perspective, these differences are significant. SKF's high proportion of fines (fibres shorter than 1 mm) could increase dust content in insulation panel production and may pose challenges in achieving the targeted material input for specific dimensions and densities. These implications established the inability of the panels with 100% SKF to achieve the target thickness (40 mm). By contrast, the fibre lengths of KF overlap more closely with the wood reference, with approximately 50% of KF fibres falling within the same size range as the wood reference fibres. However, the notable differences in the remaining fractions could influence homogeneity and the mechanical and thermal properties of the resulting panels.

The length of biomass used in this study is comparable to that examined by Khallaf, Lakbida [57], which investigated hemp shives and fibres measuring between 0.08 and 10 mm and 2 to 6 cm, respectively. This length is relatively short compared to the fibre lengths examined in the thermal insulation material studies by Sheshko, Romanovskiy [58] and El Messiry, El-Tarfawy [59], where flax fibres ranged from 5 to 10 cm. Additionally, research by Samanta, Mustafa [60] on insulation panels made from jute fibre showed length distributions between 30 mm and 300 mm.

3.2.2. DVS analysis

Fig. 7 presents the inherent hygroscopic behaviour of the biomass. The sorption properties of the materials align with the variations in chemical composition. The sorption characteristics of KF are similar to that of the wood_ref. While SKF consistently exhibited a higher equilibrium moisture content (EMC) across all relative humidity levels than KF and the wood_ref. Its high soluble content, as presented in Tables 2 and is the cause of this result. Soluble compounds, as well as pectins, contain numerous accessible hydroxyl groups, which enhance their hydrophilicity. While SKF's sorption below 60% RH appears somewhat

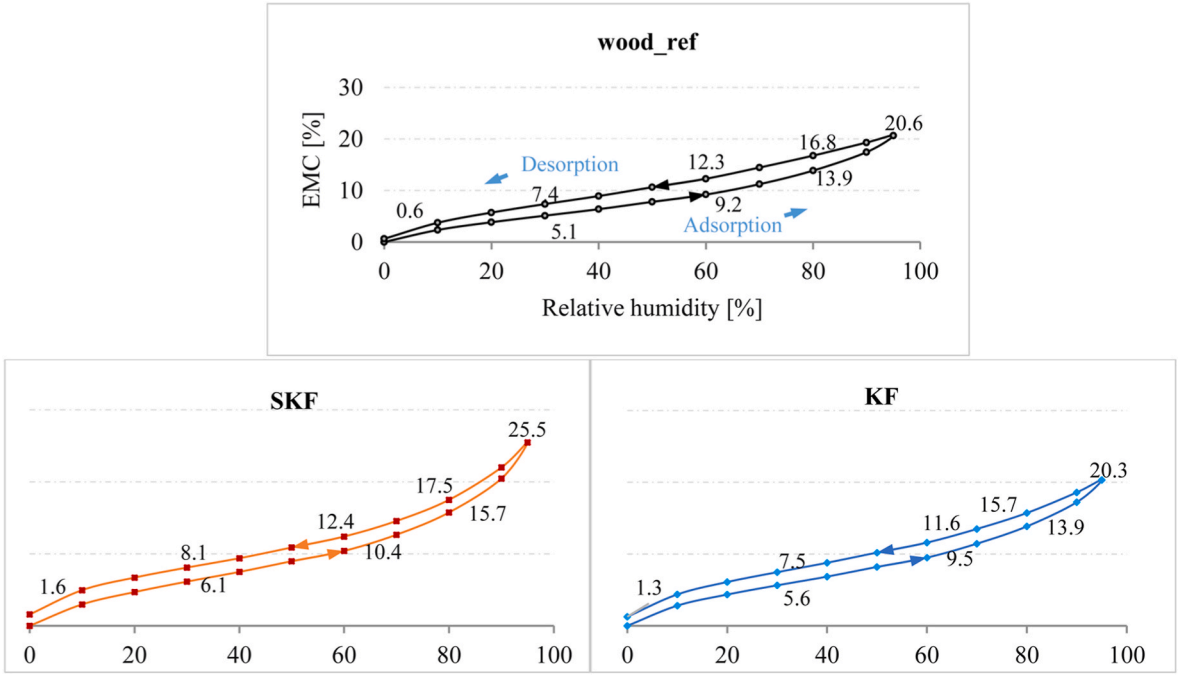

Fig. 7. Sorption hysteresis plot.

similar to the other biomass materials, a significant increase in moisture uptake was observed above this threshold. This increase may be ascribed to enhanced multilayer adsorption, capillary condensation, and potential deliquescence.

The sorption hysteresis of SKF, particularly during desorption from 95% to 80% RH, was different. SKF desorbed 8% moisture between the mentioned RH values, compared to 4.6% for KF and 3.6% for the wood_ref. This indicates that SKF retains relatively lower amount of moisture after desorption. Except at 0% RH, the wood reference consistently showed higher moisture retention than the hemp fines, while KF showed slightly less retention than SKF. This discrepancy aligns with the compositional differences presented in Tables 2 and ie., high lignin content for the wood_ref and SKF compared to KF. The higher retention for wood_ref compared to SKF is because moisture adsorbed by solubles, such as pectins, and amorphous content, such as hemicelluloses, is less firmly bound and more easily released. In contrast, lignin is significantly more hydrophobic than pectin and hemicelluloses [61]. The outcome at 0% RH highlights the implications of the presence and accessibility of a more crystalline network, such as cellulose, which would increase the potential for tightly hydrogen-bonded water. This, in combination with a high lignin content for SKF, led to a final higher moisture retention compared to KF and wood_ref. This result, relative to the initial higher adsorption for SKF, implies a greater moisture presence, which indicates that the overall moisture sorption behaviour of a lignocellulosic material depends on the interactions among its inherent complex materials.

The moisture sorption properties show that despite the lower I_c for the wood_ref, its moisture stability was higher than that of SKF. This contradicts the concluding remark from the XRD analysis and indicates that a material's overall moisture affinity is more strongly influenced by the substantial presence of soluble compounds. The high soluble content in SKF, such as pectin, significantly increased water attraction, thereby overpowering the typically lower moisture affinity of a crystalline network. The sorption activities of KF further supports this, as it performed better than SKF but was similar to the wood_ref. This provides compelling evidence that the interaction of all components of a lignocellulosic material is crucial for its overall sorption performance.

While moisture scavenging can improve indoor air quality and comfort [62], SKF's high sorption characteristics could compromise the insulation panel's dimensional stability and integrity due to swelling and shrinkage cycles [63]. Furthermore, significant moisture saturation in humid conditions, resulting from high soluble content, would reduce the panel's insulation effectiveness due to water's higher thermal conductivity compared to trapped air. This analysis is primarily indicative of the potential influence of chemical composition on sorption properties. However, it is noted that the physical structure of the insulation panel, which is affected by the size of the fines and its compactness, can also influence these properties.

3.3. Performance of the semi-rigid-hemp fines insulation panels

3.3.1. Dust content

Fig. 8 demonstrates a strong correlation between dust content in the fabricated panels and the result obtained for fibre length. Panels incorporating SKF consistently exhibited meaningfully higher dust content, approximately 3.6 times that of the baseline panels made with 100% softwood fibres, regardless of the incorporation rate (25% or 50% or 100%). This substantial dust increase in SKF panels is attributed to the limited capacity of their predominantly short fibres to intertwine and form stable, entangled networks. The similar dust content observed

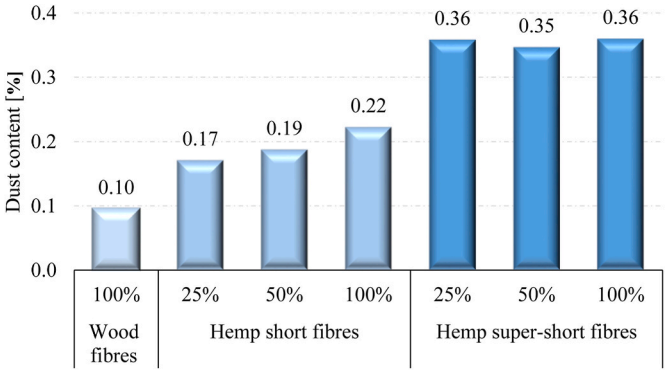

Fig. 8. Dust content.

across different SKF incorporation rates suggests a threshold or non-linear effect in dust generation. This indicates that introducing even 25% of SKF fibres was sufficient to achieve a tipping point of inter-fibre bonding disruption; consequently, increasing the proportion to 50% did not result in a proportional rise in dust. These short fibres could be easily dislodged during various stages of panel production, which inherently limits the panel's ability to effectively immobilize them. This issue led to a panel that was 28% thinner than the target. Considering that the 100% SKF panels had similar dust content to the hybrid panels, the primary reason for the thickness collapse can be ascribed to the absence of longer wood fibres that provide a scaffolding network through interlocking, overlapping, and entanglement. This high dust content, coupled with the lower thickness of the 100% SKF panel, resulted in a fragile panel with a density that deviated from the standards for semi-rigid insulation outlined in this study. Consequently, panels made exclusively with SKF were removed from further study, and the 100% super short hemp fines examined in this study were deemed unsuitable for thermal insulation panel production. In the case of hybrid batches, the presence of longer wood fibres in the panels with 25% and 50% SKF helped to provide a spring back during pressing and the internal structural integrity needed to prevent the panel from collapsing after pressing.

The panels made with KF exhibited a more favourable dust profile. A 25% loading of KF produced a dust content that was two times lower than what was observed with SKF (relative to the wood reference fibre). A 50% loading did not result in a noticeable increase in dust content. Even the panels with 100% KF fibres still produced only a twofold increase in dust content compared to the wood fibres, which was substantially lower than the results for the SKF. These 100% KF panels also met the thickness and density target. The superior performance of KF compared to SKF aligns with its fibre length distribution, which shows that 50% of its fibres are as long as the wood reference fibre. Consequently, the KF fibres have enough length to entangle or interlock with each other to form a cohesive, three-dimensional network.

3.3.2. Tensile properties

The internal bond strength performance or tensile resistance (TR) of the panels with KF was generally lower than wood reference panel, regardless of the incorporation rate (Fig. 9). A 50% incorporation of KF resulted in a notable (p-value of 0.01) 1.5-times decrease in internal bond strength performance, although it remained above the declared standard of 1 kPa (noted in Fig. 9) set by SOPREMA for semi-rigid products.

Fibre properties like length, distribution, and type significantly influence the internal bond strength of semi-rigid insulation panels. For example, longer fibres, as seen in the wood reference panel, can form a more robust interlocking network that leads to superior bonding.

Aside from the hybrid panels with 50% KF, there was no notable difference in the performance of the other panel batches compared to the wood reference. A mix of different fibre lengths, such as in the hybrid panel of SKF and wood fibres, can sometimes act synergistically to reduce stress concentration, thus improving overall bond strength (as seen with 50% SKF). This is especially true when the fines, in this case, have a sufficient aspect ratio to fill the voids within the established network, contributing to internal bond strength.

The depreciation in the case of hybrid panels with KF is likely due to inhomogeneity caused by the length of the KF fibres (as identified in section 3.1.1), which results in inadequate bridging and stress transfer. This effect is highlighted by the increasing, albeit inconsequential, reduction in performance as the fraction is increased from 25% to 50%.

In contrast, hybrid panels with short hemp fines (SKF) demonstrated internal bond strength comparable to—at a 25% incorporation rate—or slightly better than—at a 50% incorporation rate—the reference wood panels. This performance can be attributed to the shorter SKF fibres functioning more like a filler. Their high surface area and uniform distribution enhanced the overall integrity of the matrix, helping to prevent localized failures. Similar results have been reported by Kulkarni and Kishore [64], where the incorporation of fly ash as a filler reduced the tendency of fibres to cluster, leading to increased strength performance.

In a similar vein, the superior performance of the 100% KF panels over the hybrid panels can be attributed to their mitigated inhomogeneity, which resulted in a stronger structure. Nonetheless, their performance remained lower than the wood reference fibres, a disparity that may be due to the fines' length creating a less robust network compared to the reference panel's network.

3.3.3. Flame reaction

Fig. 10 shows that despite the application of FR, chemical composition likely influenced the results of flame reaction. However, all flame heights obtained meet EN ISO 11925-2 Euroclass E requirements, as no measured flame height exceeds 150 mm. Panels with 100% KF achieved substantially improved fire properties, likely due to their lower presence of volatile compounds, especially hemicelluloses.

Overall, the incorporation of SKF produced panels with the highest flame height relative to the wood reference panels, which could be due to the notably high soluble content of SKF. Solubles (pectin) and hemicelluloses are characterized by lower molecular weight compounds that undergo fast pyrolysis, which tends to increase initial flame height [65]. Despite the FR's primary interaction with these -OH rich components, the allocation of chemical resources to modify their degradation, especially when they are present in substantial quantity—depends on the flame-retardant concentration.

The inherent ignition mechanism of a biomass largely depends on the lignin content [66]. According to Hao, Chow [67], lignin resists initial thermal degradation better than cellulose and hemicelluloses because its high oxygen content and highly aromatic structure results in the production of solid char [68]. The chemical mechanism of ammonium FR salts is established to depend on the chemical composition of the biomass. For instance, the effect of ammonium salt is typically less pronounced on lignin. In contrast, the ammonium salt FR promotes the

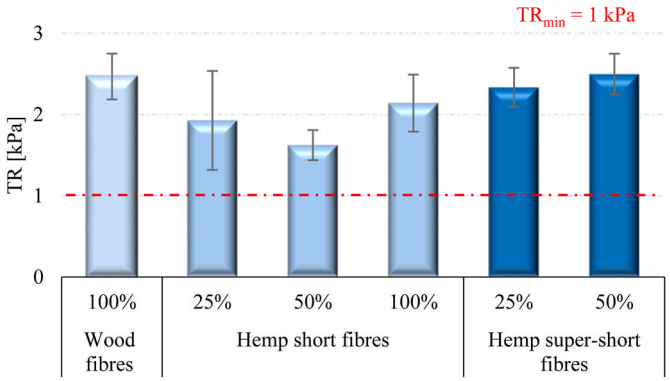

Fig. 9. Tensile test perpendicular to the grain.

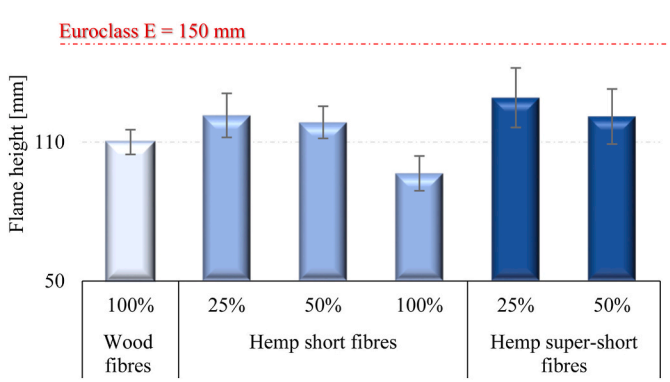

Fig. 10. Flame height.

formation of levoglucosan due to strong interaction with the -OH of the cellulose backbone. Hence, the high cellulose content appears to be the primary cause of the lower flame height of the 100% KF panel compared to the wood reference batch. Besides, hemicelluloses have been found to facilitate the degradation of cellulose [69], which may increase the release of flammable gases during the initial stages of combustion. However, even though the incorporation of ammonium salt-based FR preferentially attacks the hemicelluloses (forcing them to rapidly undergo dehydration and charring instead of pyrolysis), its overall effectiveness and nature of interaction depend on the quantity of FR used. Especially considering that the hemicelluloses in the wood biomass are notably higher compared to that in the hemp fines. This implies that in the case of KF, the potential of the FR is maximised. The reduced hemicelluloses content in the hemp, combined with the typical interactions of the char produced by crystalline cellulose and lignin, may have further restricted the release of volatiles that would otherwise have contributed to a higher flame height.

Aside from the reasons noted for the 100% batches, the partial replacement of wood fibres with hemp fines (KF or SKF) in hybrid panels results in a substantial increase in flame height (p-value$<$0.05) compared to the reference wood panel. This outcome can be attributed primarily to the effect of fibre geometry on char integrity. As discussed in other sections, the wood reference panel features long fibres that form a continuous, highly intertwined, and mechanically robust network. This structural bridging allows for a more cohesive and less permeable panel, leading to a strong char layer that restricts the escape of flammable volatile gases from the interior, thereby resulting in a lower flame height. In contrast, the shorter fines act as stress concentrators and weak points. This effect is evidenced by the TR values and is likely what occurred in the wood-KF panels, resulting in a char layer that is more porous and prone to micro-cracking and spalling (breaking away). This conclusion is further buttressed by the finding that the flame height of the 100% KF panels was lower than that of the 100% wood panels. When the char cracks, trapped flammable gases are released in a burst, feeding the flame and resulting in a higher observed flame height. Given that all panels achieved the Euroclass flame height standard, no further optimization of flame-retardant fractions is likely necessary.

3.3.4. *Thermal conductivity performance*

The thermal conductivity values for all the hybrid panels examined did not vary significantly, but they were less than that of wood_ref panel (Fig. 11). For inference, the declared thermal conductivity at 23 °C/50% HR for the wood fibre reference panel is 0.038 W/(m·K). Generally, thermal conductivity values between 0.0373 and 0.0401 W/(m·K) are considered very good for thermal insulation. Common insulators, such as mineral wool, glass fibre wool, expanded polystyrene (EPS), and extruded polystyrene (XPS), have values that fall within this range (see also Table 5). Recent research [70] also reported thermal conductivity values of 0.038 and 0.035 W/(m·K) for wood (110 kg/m^3) and EPS,

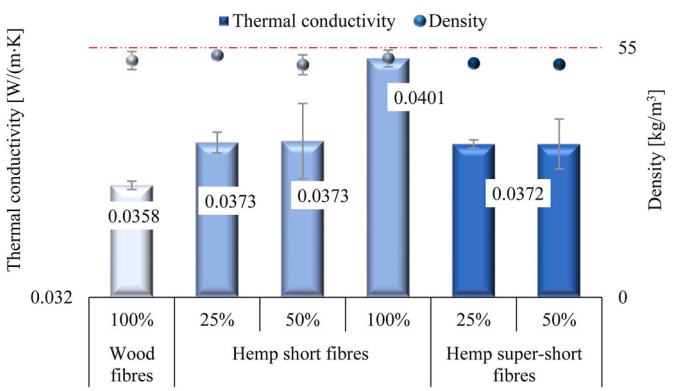

Fig. 11. Thermal conductivity relative to density.

Table 5
Properties and costs of commercial insulation materials [73, 74].

Insulation material	Kg/m^3	W/m·K	Approximate Cost, €/m^3
Rock wool	40–200	0.033–0.040	10–16.9
Glass wool	10–100	0.030–0.050	7.9–12.4
EPS	18–50	0.029–0.041	7.3–14.4
XPS	32–40	0.032–0.037	15.2–19.4
Polyurethane	30–160	0.022–0.035	21

respectively. In terms of cost, the conventional wood-based insulation panel examined in this study is priced at approximately €33.80 per m^3, which is significantly higher than traditional insulation materials shown in Table 5. By incorporating up to 25% hemp fines, a hybrid thermal insulation panel can be created that is about 13% cheaper than the wood-based insulation. Additionally, using over 50% hemp fines could lead to even lower costs compared to conventional insulation materials. Nonetheless, from an industrial viability perspective, the 0.0015 W/(m·K) depreciation observed with the hybrid panels is quite notable.

The decrease in thermal conductivity relative to the panel from wood fibre with the incorporation of hemp fines reflects the already highlighted differences in the chemical composition of the hemp fines and wood fibres. In terms of thermal insulation performance, the chemical composition of the fines can be very impactful, especially as highlighted by the higher crystallinity index for the hemp fines and the high lignin component in the wood fibres, which offers more resistance to heat transfer. The high crystallinity index provides more efficient pathways for phonons due to the presence of a denser and more ordered cellulose. Fibre size also contributes critically [71]. The study as well as Piatkiewicz, Narloch [72], highlight that fibre size affects the presence of air-filled voids that provide insulation. Shorter fibres or smaller particles lead to more solid-to-solid contact and thus increase packing, which causes a reduction in the air-filled voids necessary for thermal resistance. Therefore, the presence of shorter fibres in the hybrid panels contributed to an increase in thermal conductivity compared to the panels with the wood reference.

4. Conclusion

This study successfully repurposed hemp fines—a byproduct accounting for nearly 6% of hemp processing residue—into semi-rigid insulation panels, aligning with circular economy principles. The hemp fines consisted of super-short fibres (median length $\leq$1.6 mm} and short hemp fibres (median length $\leq$2.6 mm).

An investigation into the properties of the hemp fines revealed a complex relationship between their characteristics and resulting insulation panel performance. The super-short fine fraction was characterised by high soluble content, a strong affinity for moisture, low thermal stability, and small crystallite size. While the longer fine shows comparable characteristics to reference wood fibres, the notable multiple particle subpopulations within the short hemp batch impacted their compatibility with the wood fibres.

Completely substituting wood fibres with hemp fines appears problematic. Specifically, the super-short hemp fibres were unable to achieve the target density, thickness, and comparable thermal properties, indicating that the short size of the fines was not feasible for achieving the desired properties of the thermal insulation panels.

Despite the variations in chemical and physical properties of the investigated secondary hemp biomass, the hybrid panels generally performed comparably to the wood reference panels, with thermal conductivity values falling within the “very good” range for insulation. Notably, a 25/75 ratio of hemp fines to wood fibres proved to be the most effective combination for thermal insulation panels (thermal conductivity of roughly 0.0372 W/(m·K). However, panels with a 50% ratio, offering satisfactory performance, could be advantageous for high use of

fines and depending on applications.

This research highlights the potential for utilising hemp fines to develop sustainable, cost-effective, and competitive insulation materials. However, additional optimization is currently ongoing based on the findings in this work, and the most promising combinations are already undergoing industrial trials for pilot validation.

Submission declaration and verification

Authors declare that the work described has not been published previously, is not under consideration for publication elsewhere, and that the publication is approved by all authors and tacitly or explicitly by the responsible authorities where the work was carried out, and that, if accepted, it will not be published elsewhere in the same form, in English or in any other language, including electronically without the written consent of the copyright-holder.

All authors have read and agreed to the published version of the manuscript.

Institutional review board statement

Not applicable.

Declaration of generative AI and AI-assisted technologies in the writing process

Authors declare the use of artificial intelligence (AI) in improving grammar in the writing process. During the preparation of this work the author(s) used [Gemini (Google)] and Grammarly in order to [improve spelling and grammatical structure]. After using this tool, the author(s) reviewed and edited the content as needed and take(s) full responsibility for the content of the publication.

Funding

The work was supported by the Circular Bio-based Europe Joint Undertaking and its members and funded under the European Union Horizon-JU-CBE Project: 101112318, FIBSUN - Novel fibre value chains and ecosystem services from sustainable feed stocks (2023-2027).

CRediT authorship contribution statement

Percy Alao: Formal analysis, Investigation, Supervision, Writing – original draft, Writing – review & editing. **Maximilien Gibier:** Formal analysis, Investigation, Writing – original draft, Writing – review & editing. **Silvia Bibbo:** Data curation, Formal analysis, Investigation, Writing – review & editing. **Laurent Bedel:** Funding acquisition, Writing – review & editing. **Stergios Adamopoulos:** Conceptualization, Funding acquisition, Supervision, Writing – review & editing.

Declaration of competing interest

The authors declare that they have no known competing financial interests or personal relationships that could have appeared to influence the work reported in this paper.

Data availability

Data will be made available on request.

References

[1] D. Rutitis, et al., Sustainable value chain of industrial biocomposite consumption: influence of COVID-19 and consumer behavior, Energies 15 (2) (2022), https://doi.org/10.3390/en15020466.

[2] M. Wiprächtiger, et al., A framework for sustainable and circular system design: development and application on thermal insulation materials, Resour. Conserv. Recycl. 154 (2020), https://doi.org/10.1016/j.resconrec.2019.104631.

[3] T. Ojanen, I.P. Seppä, E. Nykänen, Thermal insulation products and applications - future road maps, Energy Proc. 78 (2015) 309–314, https://doi.org/10.1016/j.egypro.2015.11.649.

[4] L. Pérez-Lombard, J. Ortiz, C. Pout, A review on buildings energy consumption information, Energy Build. 40 (3) (2008) 394–398, https://doi.org/10.1016/j.enbuild.2007.03.007.

[5] F. Asdrubali, F. D'Alessandro, S. Schiavoni, A review of unconventional sustainable building insulation materials, Sustain. Mater. Technol. 4 (2015) 1–17, https://doi.org/10.1016/j.susmat.2015.05.002.

[6] A. Allouhi, et al., Energy consumption and efficiency in buildings: current status and future trends, J. Clean. Prod. 109 (2015) 118–130, https://doi.org/10.1016/j.jclepro.2015.05.139.

[7] B. Abu-Jdayil, et al., Traditional, state-of-the-art and renewable thermal building insulation materials: an overview, Constr. Build. Mater. 214 (2019) 709–735, https://doi.org/10.1016/j.conbuildmat.2019.04.102.

[8] Z. Wang, et al., Porous thermal insulation polyurethane foam materials, Polymers 15 (18) (2023), https://doi.org/10.3390/polym15183818.

[9] B.P. Jelle, Traditional, state-of-the-art and future thermal building insulation materials and solutions – properties, requirements and possibilities, Energy Build. 43 (10) (2011) 2549–2563, https://doi.org/10.1016/j.enbuild.2011.05.015.

[10] P. Lisowski, M.A. Glinicki, Promising biomass waste–derived insulation materials for application in construction and buildings, Biomass Convers. Biorefinery (2023), https://doi.org/10.1007/s13399-023-05192-8.

[11] C. Rojas, et al., Thermal insulation materials based on agricultural residual wheat straw and corn husk biomass, for application in sustainable buildings, Sustain. Mater. Technol. 20 (2019), https://doi.org/10.1016/j.susmat.2019.e00102.

[12] A. Bakatovich, F. Gaspar, N. Boltrushevich, Thermal insulation material based on reed and straw fibres bonded with sodium silicate and rosin, Constr. Build. Mater. 352 (2022), https://doi.org/10.1016/j.conbuildmat.2022.129055.

[13] A. Korjenic, et al., Development and performance evaluation of natural thermal-insulation materials composed of renewable resources, Energy Build. 43 (9) (2011) 2518–2523, https://doi.org/10.1016/j.enbuild.2011.06.012.

[14] A. Lakatos, Analysis of heat treatment forced thermal and structural changes of aerogel insulation blanket – a case study, Case Stud. Therm. Eng. 75 (2025), https://doi.org/10.1016/j.csite.2025.107200.

[15] Á. Lakatos, E. Lucchi, Thermal performances of Super Insulation Materials (SIMs): a comprehensive analysis of characteristics, heat transfer mechanisms, laboratory tests, and experimental comparisons, Int. Commun. Heat Mass Tran. 152 (2024), https://doi.org/10.1016/j.icheatmasstransfer.2024.107293.

[16] P. Raja, et al., A review of sustainable bio-based insulation materials for energy-efficient buildings, Macromol. Mater. Eng. 308 (10) (2023), https://doi.org/10.1002/mame.202300086.

[17] S.L. Platt, et al., Sustainable bio & waste resources for thermal insulation of buildings, Constr. Build. Mater. 366 (2023), https://doi.org/10.1016/j.conbuildmat.2022.130030.

[18] C. Pavel, D. Blagoeva, Competitive Landscape of the Eu's Insulation Materials Industry for energy-efficient Buildings, 2018, https://doi.org/10.2760/750646. Luxembourg.

[19] P. José, et al., Circular Economy: Measuring Innovation in the Product Chain, Univsersiteit Utrecht, 2017.

[20] E. Kristine, et al., Cannabis/Hemp: Sustainable Uses, Opportunities, and Current Limitations, Springer, 2022.

[21] B. Martínez, et al., Towards sustainable building solutions: development of hemp shiv-based green insulation material, Constr. Build. Mater. 414 (2024), https://doi.org/10.1016/j.conbuildmat.2024.134987.

[22] M. Degrave-Lemeurs, P. Glé, A. Hellouin de Menibus, Acoustical properties of hemp concretes for buildings thermal insulation: application to clay and lime binders, Constr. Build. Mater. 160 (2018) 462–474, https://doi.org/10.1016/j.conbuildmat.2017.11.064.

[23] M. Hussain, et al., Analysing the role of environment-related technologies and carbon emissions in emerging economies: a step towards sustainable development, Environ. Technol. 43 (3) (2022) 367–375, https://doi.org/10.1080/09593330.2020.1788171.

[24] A. Hussain, et al., Development of novel building composites based on hemp and multi-functional silica matrix, Compos. B Eng. 156 (2019) 266–273, https://doi.org/10.1016/j.compositesb.2018.08.093.

[25] D.C. Agrawal, R.K. and, M. Dhanasekaran, CannabisHemp for Sustainable Agriculture and Materials, o Springer Nature Singapore Pte Ltd, 2022, https://doi.org/10.1007/978-981-16-8778-5.

[26] E. Latif, et al., Hygric properties of hemp bio-insulations with differing compositions, Constr. Build. Mater. 66 (2014) 702–711, https://doi.org/10.1016/j.conbuildmat.2014.06.021.

[27] M.N. Kolak, M. Oltulu, Effect of expanded perlite addition on the thermal conductivity and mechanical properties of bio-composites with hemp-filled, J. Build. Eng. 71 (2023), https://doi.org/10.1016/j.jobe.2023.106515.

[28] D.M. Rivas-Aybar, et al., Assessing the techno-sustainability of hemp-based building materials: a comparative study in the Australian context, Mater. Today Sustain. 32 (2025), https://doi.org/10.1016/j.mtsust.2025.101218.

[29] T. Fiedler, J. Pedersen, Evaluating the thermal conductivity of hemp-based insulation, Materials 18 (8) (2025), https://doi.org/10.3390/ma18081723.

[30] H.M.G. van der Werf, L. Turunen, The environmental impacts of the production of hemp and flax textile yarn, Ind. Crop. Prod. 27 (1) (2008) 1–10, https://doi.org/10.1016/j.indcrop.2007.05.003.

[31] B. Klemetsrud, D. Eatherton, D. Shonnard, Effects of lignin content and temperature on the properties of hybrid poplar Bio-Oil, char, and gas obtained by fast pyrolysis, Energy & Fuels 31 (3) (2017) 2879–2886, https://doi.org/10.1021/acs.energyfuels.6b02836.
[32] X. Li, et al., Co-pyrolysis of cellulose and lignin: effects of pyrolysis temperature, residence time, and lignin percentage on the properties of biochar using response surface methodology, Ind. Crop. Prod. 219 (2024), https://doi.org/10.1016/j.indcrop.2024.119071.
[33] L. Burhenne, et al., The effect of the biomass components lignin, cellulose and hemicellulose on TGA and fixed bed pyrolysis, J. Anal. Appl. Pyrolysis 101 (2013) 177–184, https://doi.org/10.1016/j.jaap.2013.01.012.
[34] C. Moletti, et al., Hygrothermal behaviour of hemp-lime walls: the effect of binder carbonation over time, Build. Environ. (2023) 233, https://doi.org/10.1016/j.buildenv.2023.110129.
[35] Y. Abdellatef, et al., Mechanical, thermal, and moisture buffering properties of novel insulating hemp-lime composite building materials, Materials 13 (21) (2020), https://doi.org/10.3390/ma13215000.
[36] S.A. Hassanzadeh-Tabrizi, Precise calculation of crystallite size of nanomaterials: a review, J. Alloys Compd. (2023) 968, https://doi.org/10.1016/j.jallcom.2023.171914.
[37] K.S. Salem, et al., Comparison and assessment of methods for cellulose crystallinity determination, Chem. Soc. Rev. 52 (18) (2023) 6417–6446, https://doi.org/10.1039/d2cs00569g.
[38] X. Wang, et al., Effect of hot-alkali treatment on the structure composition of jute fabrics and mechanical properties of laminated composites, Materials 12 (9) (2019), https://doi.org/10.3390/ma12091386.
[39] A.D. French, M. Santiago Cintrón, Cellulose polymorphy, crystallite size, and the Segal Crystallinity Index, Cellulose 20 (1) (2013) 583–588, https://doi.org/10.1007/s10570-012-9833-y.
[40] M. Qinglin, et al., Effects of different deinking processes on fiber morphology, hydrogen bond models, and cellulose supramolecular structure, Bioresources (2013).
[41] R.H. Newman, Estimation of the lateral dimensions of cellulose crystallites using 13C NMR signal strengths, Solid State Nucl. Magn. Reson. 15 (1999) 21–29, https://doi.org/10.1016/S0926-2040(99)00043-0.
[42] S. Kiyoto, et al., Distribution of Lignin, Hemicellulose, and Arabinogalactan protein in Hemp Phloem fibers, Microsc. Microanal. 24 (4) (2018) 442–452, https://doi.org/10.1017/S1431927618012448.
[43] S.M.Q. Bokhari, K. Chi, J.M. Catchmark, Structural and physico-chemical characterization of industrial hemp hurd: impacts of chemical pretreatments and mechanical refining, Ind. Crop. Prod. 171 (2021), https://doi.org/10.1016/j.indcrop.2021.113818.
[44] J. Müssig, et al., Transdisciplinary top-down review of hemp fibre composites: from an advanced product design to crop variety selection, Composites Part C: Open Access 2 (2020), https://doi.org/10.1016/j.jcomc.2020.100010.
[45] L. Marrot, et al., Properties of frost-retted hemp fibers for the reinforcement of composites, J. Nat. Fibers 19 (17) (2021) 16017–16028, https://doi.org/10.1080/15440478.2021.1904474.
[46] K. Kafle, et al., Effects of delignification on crystalline cellulose in lignocellulose biomass characterized by vibrational sum frequency generation spectroscopy and X-ray diffraction, Bioenergy Res. 8 (4) (2015) 1750–1758, https://doi.org/10.1007/s12155-015-9627-9.
[47] N. Kontogianni, et al., Effect of alkaline pretreatments on the enzymatic hydrolysis of wheat straw, Environ. Sci. Pollut. Res. Int. 26 (35) (2019) 35648–35656, https://doi.org/10.1007/s11356-019-06822-3.
[48] I. Lawan, et al., Bio-based treatment of hemp fiber for use as reinforcement of a composite: an effort towards development of green and sustainable polybenzoxazine brake pad, Tribol. Int. 193 (2024), https://doi.org/10.1016/j.triboint.2024.109394.
[49] L. Marrot, et al., Analysis of the hemp fiber mechanical properties and their scattering (Fedora 17), Ind. Crop. Prod. 51 (2013) 317–327, https://doi.org/10.1016/j.indcrop.2013.09.026.
[50] K. Werner, L. Pommer, M. Broström, Thermal decomposition of hemicelluloses, J. Anal. Appl. Pyrolysis 110 (2014) 130–137, https://doi.org/10.1016/j.jaap.2014.08.013.
[51] G. Guerriero, et al., Transcriptomic profiling of hemp bast fibres at different developmental stages, Sci. Rep. 7 (1) (2017) 4961, https://doi.org/10.1038/s41598-017-05200-8.
[52] Y. Huang, et al., Relationships between hemicellulose composition and lignin structure in woods, J. Wood Chem. Technol. 36 (1) (2015) 9–15, https://doi.org/10.1080/02773813.2015.1039543.
[53] F. Abik, et al., Potential of wood hemicelluloses and their derivates as food ingredients, J. Agric. Food Chem. 71 (6) (2023) 2667–2683, https://doi.org/10.1021/acs.jafc.2c06449.
[54] E. Apaydın Varol, Ü. Mutlu, TGA-FTIR analysis of biomass samples based on the thermal decomposition behavior of hemicellulose, cellulose, and Lignin, Energies 16 (9) (2023), https://doi.org/10.3390/en16093674.
[55] Y. Long, et al., Interactions among biomass components during co-pyrolysis in (macro)thermogravimetric analyzers, Kor. J. Chem. Eng. 33 (9) (2016) 2638–2643, https://doi.org/10.1007/s11814-016-0102-x.
[56] J. Berglund, et al., Wood hemicelluloses exert distinct biomechanical contributions to cellulose fibrillar networks, Nat. Commun. 11 (1) (2020) 4692, https://doi.org/10.1038/s41467-020-18390-z.
[57] H. Khallaf, et al., Impact of fiber size and poly (vinyl acetate) adhesive ratio on the hygrothermal properties of non-industrial hemp-based insulation composites, Constr. Build. Mater. 494 (2025), https://doi.org/10.1016/j.conbuildmat.2025.143462.
[58] N. Sheshko, et al., Physical parameters of insulation with a structure-forming material from flax noils, E3S Web of Conferences 212 (2020), https://doi.org/10.1051/e3sconf/202021202014.
[59] M. El Messiry, et al., Development of high-performance thermal insulation panels from flax fiber waste for building insulation, J. Ind. Textil. 55 (2025), https://doi.org/10.1177/15280837251338160.
[60] K.K. Samanta, et al., Study of thermal insulation performance of layered jute nonwoven: a sustainable material, J. Nat. Fibers 19 (11) (2021) 4249–4262, https://doi.org/10.1080/15440478.2020.1856274.
[61] M.S. Ganewatta, H.N. Lokupitiya, C. Tang, Lignin biopolymers in the Age of controlled polymerization, Polymers 11 (7) (2019), https://doi.org/10.3390/polym11071176.
[62] T. Lohtander, et al., Bioactive Fiber foam films from cellulose and willow bark extract with improved water tolerance, ACS Omega 9 (7) (2024) 8255–8265, https://doi.org/10.1021/acsomega.3c08906.
[63] N. Stevulova, et al., Water absorption behavior of Hemp hurds composites, Materials 8 (5) (2015) 2243–2257, https://doi.org/10.3390/ma8052243.
[64] S.M. Kulkarni, Kishore, Effect of filler–fiber interactions on compressive strength of fly ash and short-fiber epoxy composites, J. Appl. Polym. Sci. 87 (5) (2002) 836–841, https://doi.org/10.1002/app.11501.
[65] M. Carrier, et al., Fast pyrolysis of hemicelluloses into short-chain acids: an investigation on concerted mechanisms, Energy & Fuels 34 (11) (2020) 14232–14248, https://doi.org/10.1021/acs.energyfuels.0c02901.
[66] S. Wang, et al., Effects of hemicellulose, cellulose and lignin on the ignition behaviors of biomass in a drop tube furnace, Bioresour. Technol. 310 (2020) 123456, https://doi.org/10.1016/j.biortech.2020.123456.
[67] H. Hao, C.L. Chow, D. Lau, Effect of heat flux on combustion of different wood species, Fuel 278 (2020), https://doi.org/10.1016/j.fuel.2020.118325.
[68] E. Pienihäkkinen, et al., Fast pyrolysis of hydrolysis lignin in fluidized bed reactors, Energy & Fuels 35 (18) (2021) 14758–14769, https://doi.org/10.1021/acs.energyfuels.1c01719.
[69] G. Song, D. Huang, Q. Ren, S. Hu, J. Xu, et al., Inner-particle reaction mechanism of cellulose, hemicellulose and lignin during photo-thermal pyrolysis process: Evolution characteristics of free radicals, Energy 297 (2024) 131201, https://doi.org/10.1016/j.energy.2024.131201. https://linkinghub.elsevier.com/retrieve/pii/S0360544224009745.
[70] J. Snow, B. Herzog, L. O'Brien, L. Li, Characterization of wood fiber insulation for the development of wood fiber-insulated panels (WIPs) for use in building envelope, BioResources 19 (3) (2024) 6142–6159, https://doi.org/10.15376/biores.19.3.6142-6159. https://bioresources.cnr.ncsu.edu/resources/characterization-of-wood-fiber-insulation-for-the-development-of-wood-fiber-insulated-panels-wips-for-use-in-building-envelope/. (Accessed 18 July 2024).
[71] A. Bakkour, S.-E. Ouldboukhitine, P. Biwole, S. Amziane, A review of multi-scale hygrothermal characteristics of plant-based building materials, Construction and Building Materials 412 (2024) 134850, https://doi.org/10.1016/j.conbuildmat.2023.134850. https://linkinghub.elsevier.com/retrieve/pii/S0950061823045713.
[72] W. Piątkiewicz, P. Narloch, Z. Wólczyńska, J. Mańczak, Effect of Hemp Shive Granulometry on the Thermal Conductivity of Hemp–Lime Composites, Materials 18 (15) (2025) 3458, https://doi.org/10.3390/ma18153458. https://www.mdpi.com/1996-1944/18/15/3458. (Accessed 23 July 2025).
[73] L. Lu, H. Wang, S. Yun, J. Hu, M. Wang, A state-of-the-art review of novel aerogel insulation materials for building exterior walls, Energy Sources, Part A: Recovery, Utilization, and Environmental Effects 46 (1) (2024) 16231–16252, https://doi.org/10.1080/15567036.2024.2424915. https://www.tandfonline.com/doi/full/10.1080/15567036.2024.2424915. (Accessed 24 November 2024).
[74] I. Luksta, G. Bohvalovs, G. Bazbauers, K. Spalvins, A. Blumberga, et al., Production of Renewable Insulation Material – New Business Model of Bioeconomy for Clean Energy Transition, Environmental and Climate Technologies 25 (1) (2021) 1061–1074, https://doi.org/10.2478/rtuect-2021-0080. https://www.sciendo.com/article/10.2478/rtuect-2021-0080. (Accessed 4 December 2021).